Chemistry–A European Journal | Full Paper doi.org/10.1002/chem.202102919 | Chemistry Europe European Chemical Societies Publishing

Special Collection

In Vitro and In Vivo Sequestration of Methamphetamine by a Sulfated Acyclic CB[n]-Type Receptor

Adam T. Brockett,[a] Chunlin Deng,[b] Michael Shuster,[c] Suvenika Perera,[b] Delaney DiMaggio,[b] Ming Cheng,[b] Steven Murkli,[b] Volker Briken,[c] Matthew R. Roesch,[a] and Lyle Isaacs*[b]

Dedicated to the Memory of Professor François Diederich

Abstract: We report the synthesis of two new acyclic sulfated acyclic CB[n]-type receptors (**TriM0** and **Me_4TetM0**) and investigations of their binding properties toward a panel of drugs of abuse (**1**–**13**) by a combination of ^{1}H NMR spectroscopy and isothermal titration calorimetry. **TetM0** is the most potent receptor with $K_a \geq 10^6\ M^{-1}$ toward methamphetamine, fentanyl, MDMA and mephedrone. **TetM0** is not cytotoxic toward HepG2 and HEK 293 cells below 100 μM according to MTS metabolic and adenylate kinase release assays and is well tolerated in vivo when dosed at 46 mg kg^{-1}. **TetM0** does not inhibit the hERG ion channel and is not mutagenic based on the Ames fluctuation test. Finally, in vivo efficacy studies show that the hyperlocomotion of mice treated with methamphetamine can be greatly reduced by treatment with **TetM0** up to 5 minutes later. **TetM0** has potential as a broad spectrum in vivo sequestrant for drugs of abuse.

Introduction

The abuse of prescription and illicit drugs is a national emergency in the United States that results in a large number of deaths annually due to overdose.[1] It is estimated that the costs of healthcare and decreased work productivity associated with drug abuse exceeds $271 billion per year and that 10.2% of the population over age 12 use illicit drugs each month.[2] The most commonly abused drugs include opioids (e.g. heroin), non-opioids (e.g. methamphetamine, cocaine), hallucinogens (e.g. ketamine and phencyclidine), marijuana, and prescription medicines. Accordingly, there is a pressing need to develop therapeutics to treat drug overdose across the full range of drugs of abuse. Overdose with opioids can currently be counteracted by treatment with Naloxone which acts by a *pharmacodynamic* effect at the opioid receptor.[3] However, Naloxone is not effective in treating patients that have overdosed on methamphetamine, cocaine, phencyclidine or ketamine.[4] Furthermore, Naloxone is less effective at treating high potency synthetic opioids like fentanyl and carfentanil.[5] An alternative class of methods to treat drug abuse and overdose relies on *pharmacokinetic* approaches which decrease the concentration of freely circulating drug by catalytic destruction or non-covalent sequestration.[3] For example, human butyrylcholine esterase catalytically transforms cocaine to ecgonine methyl ester and is therefore explored as a therapeutic for cocaine intoxication.[6] Conversely, antibodies can be raised that bind tightly to methamphetamine, cocaine, and fentanyl. Such antibodies sequester drugs in the bloodstream, prevent their passage through the blood brain barrier, and therefore can be used to combat drug abuse and overdose.[7] As supramolecular chemists, we envisioned that high affinity macrocyclic hosts (Figure 1) could enable a complementary pharmacokinetic approach to combat death due to drug overdose by sequestering drugs of abuse in vivo as their macrocycle–drug complexes.[8]

Supramolecular chemists seek to understand the nature of non-covalent interactions, create new supramolecular recognition systems, and use them to enable new chemical and biological applications.[9] Preorganized macrocyclic hosts lie at the heart of supramolecular chemistry because they often display high affinity and highly selective interactions with their targets.[9c] Cyclodextrins, calixarenes, cavitands, cyclophanes, cucurbit[n]urils (CB[n]), and pillararenes are among the most commonly studied macrocyclic host systems.[9c,10] Guest compounds that are encapsulated within the cavity of macrocyclic

[a] Dr. A. T. Brockett, Prof. Dr. M. R. Roesch
Department of Psychology and Program in Neuroscience and Cognitive Science (NACS)
University of Maryland at College Park, College Park, MD 20742 (United States)

[b] Dr. C. Deng, S. Perera, D. DiMaggio, Dr. M. Cheng, Dr. S. Murkli, Prof. Dr. L. Isaacs
Department of Chemistry and Biochemistry
University of Maryland at College Park, College Park MD 20742 (United States)
E-mail: LIsaacs@umd.edu

[c] M. Shuster, Prof. Dr. V. Briken
Department of Cell Biology and Molecular Genetics
University of Maryland at College Park, College ParkMD 20742, United States

Supporting information for this article is available on the WWW under https://doi.org/10.1002/chem.202102919

Special Collection This article belongs to a Joint Special Collection dedicated to François Diederich.

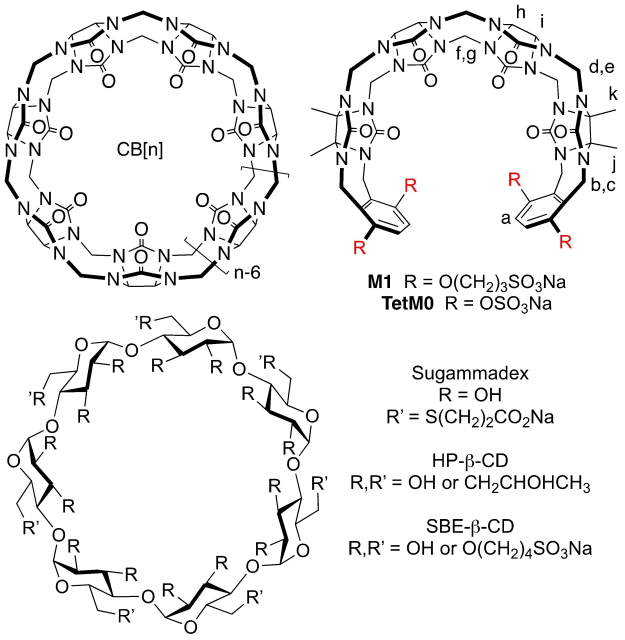

Figure 1. Structure of CB[n], acyclic CB[n]-type receptors **M1** and **TetM0**, and Sugammadex.

hosts often display different physical properties, photophysical properties, chemical reactivity, and biological properties than the uncomplexed guest compound. Accordingly, popular in vitro application of macrocycles include sensing ensembles,[11] supramolecular catalysts,[12] supramolecular materials,[13] chiral separations phases,[14] household deodorizers,[15] and molecular machines.[9d,16] Many classes of macrocyclic hosts display high binding affinity in buffered water and are biocompatible which enables in vivo applications. For example, sulfonated calix[4]arene can be used to reduce the in vivo (mice) toxic effects of methyl viologen.[17] Recently, water soluble pillararenes have been investigated as in vivo reversal agents for neuromuscular blockers.[18] Squaraine rotaxanes have been used for in vivo imaging and theragnostic applications.[19] Most significantly, cyclodextrin derivatives (Figure 1) are currently widely used in several real world applications. For example, SBE-β-CD is widely used as a solubilizing excipient for insoluble drugs for parenteral administration to humans,[20] HP-β-CD is the active ingredient in the household product Febreeze™,[15b] and Sugammadex is used clinically as an in vivo reversal agent for the post-operative side effects of the neuromuscular blocking agents rocuronium and vecuronium.[8d,21]

We, and others, have been interested in the synthesis and molecular recognition properties of an alternative class of molecular container compounds known as cucurbit[n]urils (CB[n], Figure 1).[10h,22] CB[n] are composed of *n* glycoluril units connected by *2n* methylene bridges that define a central hydrophobic cavity and two symmetry equivalent electrostatically negative ureidyl carbonyl portals. Accordingly, CB[n] hosts display ultra-high affinity toward hydrophobic (di)cations in aqueous solutions with K_a values reaching 10^{17} M^{-1} in special cases.[23] Among the unfunctionalized macrocyclic CB[n] (n = 5, 6, 7, 8, 10), CB[7] is most actively investigated due to its good water solubility (> 5 mM), excellent biocompatibility, and its sizable cavity which can accommodate a variety of biologically active guests.[24] The Wang group has used CB[7] as an in vivo antidote to counteract the effects of paraquat poisoning,[25] to alleviate blood coagulation induced by hexadimethrine bromide (mice),[26] to reverse paralysis induced by succinyl choline (mice),[18a] and to reverse general anesthesia in zebrafish.[27] Recently, we demonstrated that a water soluble derivative of CB[8] was able to sequester phencyclidine (PCP) in vivo (mice) and thereby control their hyperlocomotion.[28] In a related line of inquiry, we and others, have synthesized acyclic CB[n]-type receptors (e.g. **M1**, Figure 1) that feature a central glycoluril oligomer, two aromatic sidewalls, and four propanesulfonate solubilizing sidearms.[29] In a series of papers we established the influence of the glycoluril oligomer length, sidewall identity, and solubilizing group identity on host binding affinity.[30] Acyclic CB[n] retain the essential molecular recognition properties of macrocyclic CB[n], display high water solubility and outstanding biocompatibility, and allow straightforward functionalization to tailor binding affinity and selectivity.[29a] Previously, we have demonstrated that **M1** and analogues function as solubilizing agents for insoluble drugs and as in vivo reversal agents for neuromuscular blockers (rocuronium, vecuronium, cistracurium), anesthetics, and drugs of abuse (e.g. methamphetamine and fentanyl).[8a,31] Most recently, we reported the synthesis of **TetM0** which is formally derived from **M1** by the deletion of the $(CH_2)_3$ linkers between the sidewalls and the SO_3^- moieties to create sulfate substituents.[32] This structural change brings the anionic groups closer to the ureidyl carbonyl portals and enhances binding affinity toward selected (di)cationic guests (e.g. rocuronium). In this paper, we synthesize new acyclic CB[n] sulfates, measure their binding affinity toward a panel of drugs of abuse (Figure 2), and demonstrate the ability of **TetM0** to control the hyperlocomotion of mice that had been treated with methamphetamine.

Results and Discussion

This results and discussion section is subdivided into sections as follows. First, we report the synthesis of two new acyclic CB[n] sulfates (**TriM0** and **Me_4TetM0**). Subsequently, we investigate the binding properties of **TetM0**, **TriM0**, and **Me_4TetM0** toward a panel of 13 drugs of abuse (Figure 2) by means of ^{1}H NMR spectroscopy and isothermal titration calorimetry (ITC). Next, we demonstrate in vitro and in vivo biocompatibility (cytotoxicity and maximum tolerated dose) of **TetM0** as well as its lack of mutagenicity (Ames test) and hERG ion channel inhibitory activity. Finally, in vivo efficacy studies show that **TetM0** is capable of controlling the hyperlocomotion of mice dosed with methamphetamine.

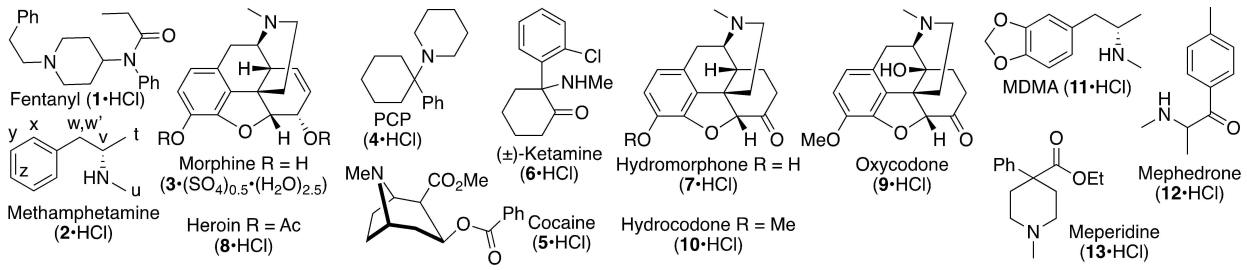

Figure 2. Chemical structures of drugs of abuse (**1**–**13**) used in this study.

Synthesis of TriM0 and Me_4TetM0

We have previously reported the synthesis of **TetM0** (Figure 1) by the double electrophilic aromatic substitution reaction of glycoluril tetramer bis(cyclic ether) (**TetBCE**) with hydroquinone followed by sulfation with py·SO_3 in hot pyridine.[32] Scheme 1 shows the synthesis of **TriM0** and **Me_4TetM0** by an analogous synthetic route. For the synthesis of **TriM0**, we begin with the reaction of glycoluril trimer bis(cyclic ether) **TriBCE**[30a] with hydroquinone (4 equiv.) in trifluoroacetic acid (TFA) at 25 °C to deliver **TriMOH** in 80% yield (Scheme 1). Subsequent reaction of **TriMOH** with py·SO_3 in hot pyridine (90 °C) gave **TriM0** in 55% yield. **TriM0** was fully characterized by ^{1}H and ^{13}C NMR, IR, and mass spectrometry (Supporting Information). The ^{1}H and ^{13}C NMR spectra of **TriM0** display 8 and 12 resonances, respectively, which are in accord with their depicted C_{2v}-symmetric structures. For the preparation of **Me_4TetM0**, we reacted tetramer bis(cyclic ether) **TetBCE** with 2,3-dimethylhydroquinone (**Me_2HQ**) in TFA to give **Me_4TetMOH** in 43% yield as an insoluble cream colored solid. Sulfation of **Me_4TetMOH** was performed in hot pyridine using py·SO_3 to deliver **Me_4TetM0** in 87% yield. Host **Me_4TetM0** was fully characterized by ^{1}H and ^{13}C NMR, IR, and mass spectrometry (Supporting Information). For example, the ESI-MS spectrum of **Me_4TetM0** shows an ion at *m/z* 691 which corresponds to **Me_4TetM0^{2-}**. The ^{1}H and ^{13}C NMR spectra recorded for **Me_4TetM0** show 11 and 15 resonances, respectively, as expected based on the depicted C_{2v}-symmetry.

Qualitative ^{1}H NMR host guest recognition study

First, we performed ^{1}H NMR dilution experiments (5 mM to 100 μM) which show that **TriM0** and **Me_4TetM0** do not undergo self-association in buffered water (Supporting Information). Next, we performed qualitative host–guest binding studies between the three hosts (**TetM0**, **TriM0**, **Me_4TetM0**) and the drugs of abuse panel (**1**–**13**, Figure 2). In these studies, we prepared mixtures of host and guest at 1:1 and 1:2 ratio and monitored the changes in chemical shift to glean information regarding the symmetry and geometry of the host–guest complex and the rate of guest exchange relative to the ^{1}H NMR chemical shift timescale. Figure 3 shows NMR spectra recorded for the interaction between hosts **TetM0**, **TriM0**, and **Me_4TetM0** and methamphetamine as guest. Figure 3a,b,c,g show the ^{1}H NMR spectra for the interaction of **TetM0** with methamphetamine which display a number of interesting features. For example, upon formation of the **TetM0**·methamphetamine complex (Figure 3b), the resonance for aryl resonance H_a of **TetM0** shifts upfield and becomes split into a pair of coupled doublets. This splitting into a pair of doublets reflects the fact that methamphetamine is chiral and C_1-symmetric and therefore all protons in the **TetM0**·methamphetamine complex are different along with the fact that the ammonium ion can reside at either ureidyl C=O portal by 180 degree rotation of **TetM0**. Similarly, the resonances for the methylene bridges of the glycoluril oligomer (e.g. H_b, H_d, and H_f; H_c, H_e, and H_g) split into two sets of five resonances that reflects the reduced effective symmetry of the **TetM0**·methamphetamine complex (Fig-

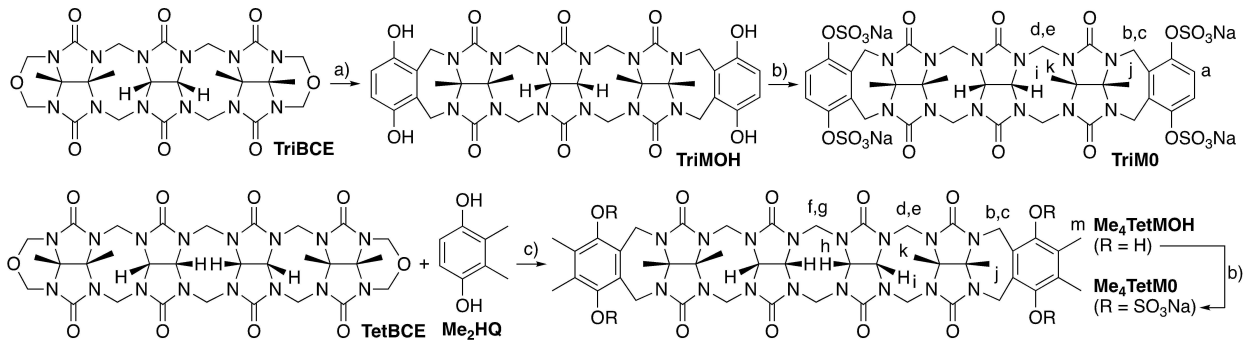

Scheme 1. Synthesis of new sulfated acyclic CB[n]-type receptors **TriM0** and **Me_4TetM0** used in this study. Conditions: a) TFA, hydroquinone (4 equiv.), RT, 80%; b) pyridine, py·SO_3, 90 °C; c) TFA, **Me_2HQ** (4 equiv.), RT, 43%.

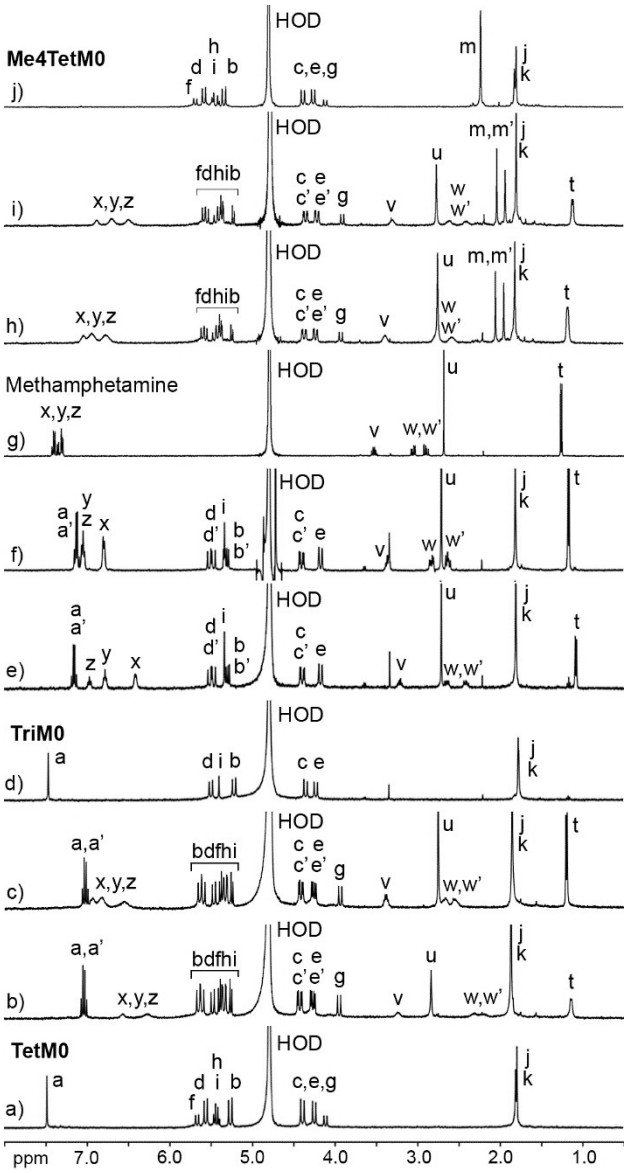

Figure 3. ^{1}H NMR spectra recorded (400 MHz, RT, D_2O) for: a) **TetM0** (1 mM), b) an equimolar mixture of **TetM0** and methamphetamine (1 mM), c) a mixture of **TetM0** (1 mM) and methamphetamine (2 mM), d) **TriM0** (1 mM), e) an equimolar mixture of **TriM0** and methamphetamine (1 mM), f) a mixture of **TriM0** (1 mM) and methamphetamine (2 mM), g) methamphetamine (0.5 mM), h) a mixture of **Me_4TetM0** (0.5 mM) and methamphetamine (1.0 mM), i) a mixture of **Me_4TetM0** (0.5 mM) and methamphetamine (0.5 mM), and j) **Me_4TetM0** (0.5 mM).

ure 3b). The resonances for the aryl (H_x, H_y, H_z) and methylene (H_w, $H_{w'}$) resonances of methamphetamine undergo significant upfield shifts which establishes that the aryl ring of methamphetamine binds inside the cavity of **TetM0** as previously established crystallographically for **M1**.[8a] The broadening of the H_x–H_z resonances (Figure 3b) indicates that the rate of guest exchange is in the intermediate exchange regime on the chemical shift timescale. At a 1:2 **TetM0**:methamphetamine ratio, the resonances for H_x–H_z shift back toward the chemical shift observed for uncomplexed methamphetamine (Figure 3g) which further establishes the intermediate nature of the exchange process and the 1:1 host–guest stoichiometry (see below). Similar changes are observed during the complexation of **TriM0** with methamphetamine (Figure 3d,e,f,g). Notably, the resonances for H_x–H_z of **TriM0**·methamphetamine (Figure 3e and 3f) appear as sharp resonances that display the expected coupling (one doublet and two triplets) which establish fast guest exchange on the chemical shift timescale. Fast guest exchange is often observed for weaker host–guest complexes as a consequence of the fact that $K_a = k_{on} / k_{off}$ and k_{on} is usually diffusion limited. Finally, the ^{1}H NMR spectra for the interaction of **Me_4TetM0** with methamphetamine are shown in Figure 3g–3j which display similar changes in chemical shift due to desymmetrization of upon host–guest complexation and inclusion of the aryl ring of methamphetamine in the cavity of **Me_4TetM0**. As expected, the CH_3-groups (H_m) of **Me_4TetM0** split into two singlets upon formation of **Me_4TetM0**·methamphetamine. Related ^{1}H NMR investigations were performed for the remaining 12 remaining guests with **TetM0**, **TriM0**, and **Me_4TetM0** and are reported in the Supporting Information. As expected, the hydrophobic region of each guest is bound within the host cavity which positions the ammonium cation at the carbonyl portal of the host. The ^{1}H NMR results obtained with methamphetamine, fentanyl, MDMA, and mephedrone indicate that the (substituted) phenethylammonium ion moiety is a privileged binding site for acyclic CB[n]-type receptors that is also found in a variety of synthetic opioids which suggests the use of (sulfated) acyclic CB[n] as broad spectrum sequestering agents.

Measurement of the thermodynamic parameters of complex formation by ITC

After elucidating the geometry and dynamic properties of the host–drug complexes by ^{1}H NMR spectroscopy, we turned our attention toward measuring their thermodynamics of complexation. Given the previously established tight binding of **TetM0** toward diammonium guests like rocuronium, the limited dynamic range of ^{1}H NMR titrations (e.g. $\leq 10^4$ M^{-1}), and our desire to use a single analytical method to determine all the binding constants lead us to use isothermal titration calorimetry. In ITC, a solution of the host in the ITC cell is titrated with a solution of guest in the ITC syringe and the heat evolved is monitored, integrated, and can be fitted to the one set of sites binding model with $n = 1$ (hereafter referred to as a 1:1 binding model) to obtain K_a, ΔH, and host–guest stoichiometry.[33] For example, Figure 4a shows a plot of DP versus time when a solution of **TetM0** (100 μM) in the ITC cell was titrated with a solution of MDMA (1 mM) in the syringe. Figure 4b shows a plot of ΔH versus molar ratio that was fitted to the 1:1 binding model in the PEAQ ITC data analysis software to extract $K_a = (2.54 \pm 0.21) \times 10^6$ M^{-1} and $\Delta H = (-17.8 \pm 0.13)$ kcal mol^{-1}. Related direct ITC titrations were performed for the remainder of the complexes between hosts **TetM0**, **TriM0**, and **Me_4TetM0** and the panel of drugs of abuse. The experimental data are presented in the Supporting Information and the thermodynamic data is summarized in Table 1. In these ITC experiments,

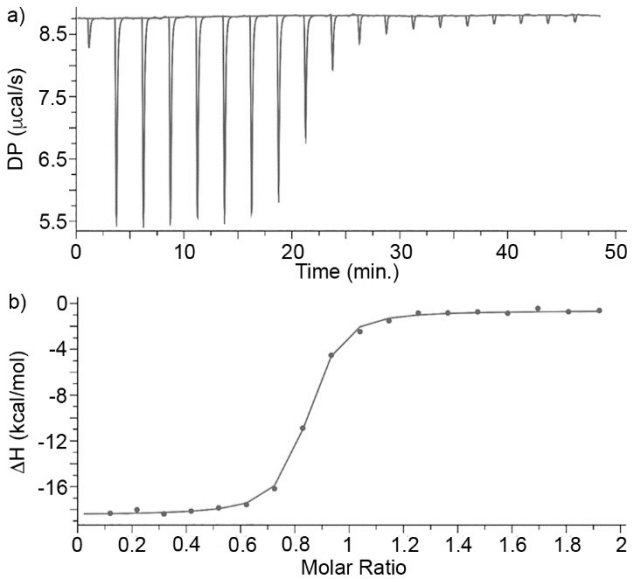

Figure 4. a) Plot of DP vs. time from the titration of **TetM0** (100 μM) in the cell with **MDMA** (1.0 mM) in the syringe in 20 mM NaH_2PO_4 buffer (pH = 7.4); b) plot of ΔH as a function of molar ratio of **TetM0** to **MDMA**. The solid line represents the best non-linear fit of the data to a 1:1 binding model with $K_a = (2.54 \pm 0.21) \times 10^6\ M^{-1}$ and $\Delta H = (-17.8 \pm 0.13)$ kcal mol^{-1}.

we maintained the *c*-value ($c = K_a \times$ [host]) lower than 500 which is recommended to ensure the accuracy of direct ITC titrations.[34]

The results in Table 1 show that the host·drug binding affinity spans from $2.66 \times 10^3\ M^{-1}$ for **TriM0**·ketamine to $3.64 \times 10^6\ M^{-1}$ for **TetM0**·fentanyl. All of the host·drug complexes are driven by favorable changes in enthalpy. The enthalpic driving force for these complexation events results from the non-classical hydrophobic effect which derives from the presence of high energy waters in the cavity of uncomplexed host that are released upon host·drug complexation as has been established previously for cyclophanes and macrocyclic CB[n] hosts.[35] The data in Table 1 allow a comparison of the binding efficiency of hosts that differ in the length of the glycoluril oligomer (e.g. **TetM0** *versus* **TriM0**) and separately between hosts with different sidewalls (e.g. **TetM0** versus **Me_4TetM0**). Table 1 establishes that **TetM0** binds 2.1 to 1724-fold more tightly than **TriM0** does toward a specific drug. We surmise that the cavity of **TriM0** which is shaped by only three glycoluril rings is smaller than that of **TetM0** which is shaped by four glycoluril rings and therefore undergoes less powerful non-classical hydrophobic binding.[35b] Additionally, the portal of **TriM0** contains fewer ureidyl C=O groups than **TetM0** which results in weaker ion-dipole interactions between **TriM0** and drug. Related results have been previously observed during the use of **M1** and its glycoluril trimer based analogue as a solubilizing excipient for insoluble drugs.[30a] Table 1 also allows us to discern the influence of the four methyl groups on the aromatic walls of **Me_4TetM0** on the binding affinity toward a common drug relative to that measured for **TetM0**. A priori, one might expect that the longer aromatic sidewalls of **Me_4TetM0** might expand the cavity due to sidewall···sidewall interactions which could result in more powerful non-classical hydrophobically driven binding. Experimentally, we find that **TetM0** is a comparable to slightly more potent host for a given drug than **Me_4TetM0** by factors of 0.57 to 10.7-fold. The selectivities of **TetM0** versus **Me_4TetM0** for the narrower guests methamphetamine, fentanyl, MDMA and mephedrone range from 4.6 to 9.7 which probably reflects the fact the cavity of **TetM0** is properly sized for the (substituted) phenethylammonium ion moiety. In previous studies, we observed that **Me_4M1** was a less efficient solubilizing excipient than **M1**.[30b] Given that **TetM0** is the most powerful host with highest potential as an in vivo sequestrant, a discussion of its binding preferences is warranted. **TetM0** binds with submicromolar dissociation constants fentanyl, methamphetamine, MDMA, and mephedrone. These four drugs each feature a narrow arylethyl ammonium ion binding epitope which is complementary to acyclic CB[n]-type receptors cavity shaped by four glycolurils. Furthermore, **TetM0** displays submicromolar affinity toward hydromorphone and hydrocodone which feature larger but more hydrophobic polycyclic skeletons. Here, the known ability of acyclic CB[n] to expand their cavity in

Table 1. Thermodynamic parameters (K_a (M^{-1}), $\triangle H^\circ$ (kcal mol^{-1}) determined for the complexes of **TetM0**, **TriM0**, and **Me_4TetM0** with the panel of drugs of abuse by direct ITC titrations. Conditions: 20 mM NaH_2PO_4 buffered water (pH = 7.4), 298 K.

Guest (G)	TetM0 K_a [M^{-1}]	$\triangle H^\circ$ [kcal/mol]	TriM0 K_a [M^{-1}]	$\triangle H^\circ$ [kcal/mol]	Me_4TetM0 K_a [M^{-1}]	$\triangle H^\circ$ [kcal/mol]
Fentanyl (**1**)	3.64×10^6 [a]	-12.2 ± 0.08 [a]	$(3.23 \pm 0.19) \times 10^4$	-4.47 ± 0.09	$(4.80 \pm 0.26) \times 10^5$	-18.4 ± 0.16
Methamphetamine (**2**)	$(2.49 \pm 0.14) \times 10^6$	-8.94 ± 0.06	$(3.44 \pm 0.09) \times 10^3$	-4.99 ± 1.03	$(2.57 \pm 0.20) \times 10^5$	-10.5 ± 0.19
Morphine (**3**)	$(7.69 \pm 0.46) \times 10^5$	-8.03 ± 0.06	$(4.46 \pm 0.43) \times 10^3$	-2.36 ± 0.19	$(2.02 \pm 0.10) \times 10^5$	-20.5 ± 0.21
Phencyclidine (PCP, **4**)	$(1.63 \pm 0.14) \times 10^5$	-6.26 ± 0.14	$(1.97 \pm 0.08) \times 10^4$	-2.98 ± 0.04	$(1.68 \pm 0.09) \times 10^5$	-6.79 ± 0.10
Cocaine (**5**)	$(2.01 \pm 0.32) \times 10^5$	-18.9 ± 0.75	$(1.49 \pm 0.74) \times 10^4$	-3.88 ± 0.09	$(2.23 \pm 0.08) \times 10^5$	-11.6 ± 0.08
Ketamine (**6**)	$(8.13 \pm 1.6) \times 10^3$	-12.1 ± 2.36	$(2.66 \pm 1.36) \times 10^3$	-5.68 ± 1.86	$(1.08 \pm 0.05) \times 10^4$	-6.34 ± 0.11
Hydromorphone (**7**)	$(2.54 \pm 0.54) \times 10^6$	-15.4 ± 0.36	n.d.	n.d.	n.d.	n.d.
Heroin (**8**)	$(8.20 \pm 0.35) \times 10^5$	-14.5 ± 0.08	$(4.81 \pm 1.15) \times 10^3$	-2.87 ± 0.43	$(7.63 \pm 0.78) \times 10^4$	-7.62 ± 0.17
Oxycodone (**9**)	$(3.24 \pm 0.57) \times 10^6$	-19.4 ± 0.35	$(5.05 \pm 1.32) \times 10^3$	-7.80 ± 1.24	$(1.01 \pm 0.20) \times 10^6$	-12.3 ± 0.32
Hydrocodone (**10**)	$(8.40 \pm 0.96) \times 10^5$	-12.7 ± 0.27	$(2.67 \pm 0.04) \times 10^3$	-1.66 ± 0.21	$(1.47 \pm 0.67) \times 10^6$	-17.4 ± 0.94
MDMA (**11**)	$(2.54 \pm 0.21) \times 10^6$	-17.8 ± 0.13	$(7.35 \pm 0.69) \times 10^3$	-5.13 ± 0.26	$(4.63 \pm 0.58) \times 10^5$	-11.1 ± 0.24
Mephedrone (**12**)	$(1.24 \pm 0.08) \times 10^6$	-16.4 ± 0.13	$(6.45 \pm 0.82) \times 10^3$	-5.82 ± 0.40	$(2.67 \pm 0.31) \times 10^5$	-11.4 ± 0.31
Meperidine (**13**)	$(9.09 \pm 1.9) \times 10^3$	-9.08 ± 1.57	$(4.27 \pm 0.24) \times 10^3$	-2.53 ± 0.08	$(1.06 \pm 0.05) \times 10^4$	-6.32 ± 0.11

[a] Taken from the literature.[32] n.d. = not determined.

a low energy cost process by flexing their methylene bridged glycoluril oligomer backbone plays an important role. Overall, we find that **TetM0** displays excellent affinity toward methamphetamine, synthetic opioids (e.g. fentanyl and derivatives), and opioids (e.g. oxycodone) which suggests that **TetM0** should be considered as a general purpose in vivo sequestrant.

In vitro cytotoxicity and in vivo maximum tolerated dose studies

Given the submicromolar dissociation constants displayed by **TetM0** described above, we decided to proceed toward its use as an in vivo sequestrant. As a first step, we wanted to assess the in vitro and in vivo biocompatibility of **TetM0**. Initially, we performed the MTS cell viability and the adenylate kinase (AK) release cell death assays with **TetM0** (Figure 5). We performed the in vitro cytotoxicity tests using human kidney (HEK 293) and human liver (HepG2) cells because they report on potential kidney and liver toxicity which are relevant since compounds accumulate in these organs for processing and clearance. The cell lines HEK293 (CRL-1573) and HepG2 (HB-8065) were purchased from ATCC. In the MTS assay, untreated (UT) cells were set to 100% cell viability, whereas in the AK release assay distilled water (W) was used as a positive control (100% release). Figure 5a,b show that HepG2 and HEK 293 cells treated with **TetM0** show a dose dependent change in cell viability. At the highest dose (1 mM) statistically significant decrease in cell viability were seen; HepG2 cells showed an 80% reduction whereas HEK 293 cells showed a 55% decrease. At [**TetM0**] $\leq$ 100 μM, no statistically significant differences in cell viability were observed. Figure 5c,d show the results of the AK release assay. Even at the highest dose tested (1 mM) neither HepG2 nor HEK 293 cells show any statistically significant increases in cell lysis relative to distilled water as positive control.

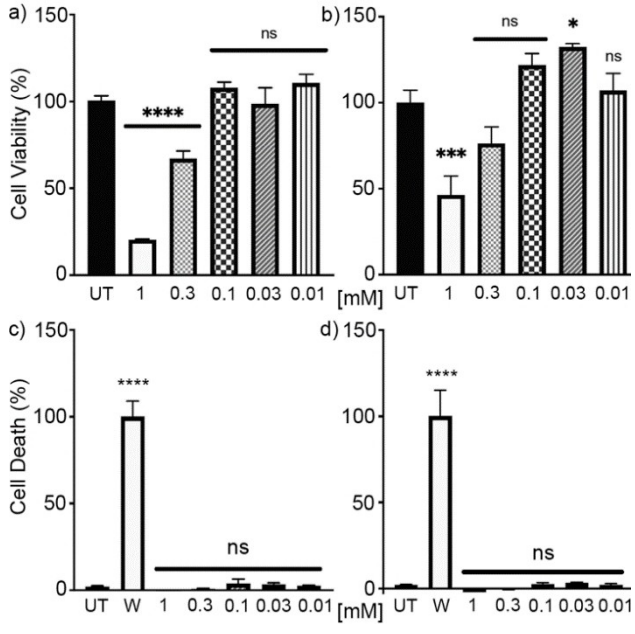

Figure 5. In vitro cytotoxicity experiments performed for **TetM0**. a) HepG2 cell viability assay after incubating the cells with **TetM0** for 24 h. b) HEK 293 cell viability assay performed after incubation with **TetM0** for 24 h. c) HepG2 cell death after incubation with **TetM0**. d) HEK 293 cell death after incubation with **TetM0**. The AK assays in panels c and d were performed using the supernatant from cells seeded for MTS assay. All panels of the figure show the average and SEM values from two replicate experiments. Statistical analysis is one-way ANOVA with Dunnett's multiple comparisons test. UT = untreated; *P = 0.01–0.05; **P = 0.001–0.01; ***P = 0.001–0.0001; ****$P < 0.0001$.

After demonstrating the low cytotoxicity of **TetM0** at concentrations below 100 μM, we proceeded to perform an in vivo maximum tolerated dose study (Figure 6). For this study, we formulated **TetM0** in 5% aqueous dextrose (D5 W) because the solubility of **TetM0** was low in PBS. Female Swiss Webster mice were divided into three treatment groups (n = 5, [**TetM0**] = 10, 8, 6 mM) and a control group (n = 5) that received only D5 W. The mice were dose via tail vein injection (0.150 mL) on days 0 and 2 (denoted by *). The mice were weighed every other day and monitored for changes in behavior and health status. Figure 6 shows that the weight of the animals receiving the highest **TetM0** dose was comparable to those receiving D5 W. However, mice receiving [**TetM0**] = 10 mM (83 mg kg^{-1}) showed visual signs of adverse behavior including labored breathing, reduced locomotion, and reduced socialization for about 20 minutes after injection. These effects were not observed in the group receiving [**TetM0**] = 6 mM (46 mg kg^{-1}). Accordingly, the concentration of **TetM0** for the planned in vivo efficacy study was set at 6 mM. All animal experiments were approved by the University of Maryland Animal Care and Use Committee (R-JAN-17-25 and RAUG-18-42) and conformed to the guidelines set forth by the National Research Council committee for the Update of the Guide for the Care and Use of Laboratory Animals.

hERG ion channel inhibition

The hERG ion channel is a voltage-gated potassium channel in cardiac cells that is essential for cardiac repolarization. When the hERG ion channel is inhibited, the electrical depolarization

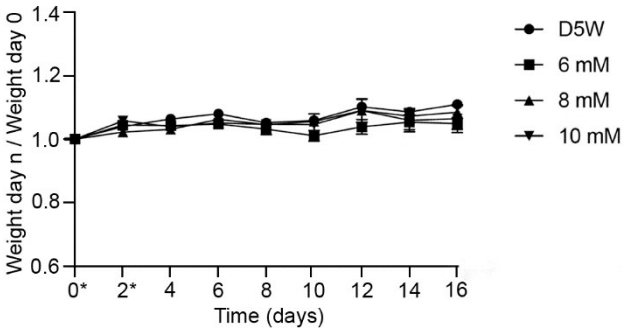

Figure 6. MTD study performed for **TetM0**. Female Swiss Webster mice (n = 5 per group) were dosed via tail vein injection (0.150 mL) on days 0 and 2 (denoted by *) with different concentrations of **TetM0** or 5% aqueous dextrose (D5 W). The normalized average weight change per study group is indicated. Error bars represent SEM.

and repolarization of the heart ventricles is extended, leading to potentially fatal cardiac malfunction. Accordingly, new chemical entities are typically screened for hERG ion channel inhibition early in the drug development process.[36] The ability of **TetM0** to inhibit the hERG ion channel (six concentrations from 0.008 μM to 25 μM) was evaluated via the patch-clamp technique (QPatch HTX). The patch clamp hERG assay was conducted using mammalian cells (HEK 293) expressing the hERG ion channel. Figure 7 shows the results of the hERG assay for **TetM0** and for E-4031 as positive control. As can be readily seen, the positive control (E-4031) exhibits a sharp increase in inhibition of ion channel activity as the concentration increases past 0.01 μM. In contrast, no concentration dependent change in ion channel activity is observed for the cells treated with **TetM0**. The calculated IC_{50} value for E-4031 is 0.0267 μM whereas the IC_{50} value for **TetM0** is greater than 25 μM. IC50 values below 0.1 μM are defined as highly potent inhibitors of the hERG channel, values between 0.1 and 1 μM as potent, values between 1–10 μM as moderately potent, and finally, IC50 values above 10 μM are typically categorized as having little to no inhibition of the channel.[37] Accordingly, **TetM0** is not an inhibitor of the hERG ion channel which encourages the further development of the in vivo sequestering abilities of **TetM0**.

Ames fluctuation assay

To assess the potential genotoxicity of **TetM0**, the Ames fluctuation test and the associated bacterial cytotoxicity assays were performed. The Ames fluctuation test is a reverse mutation assay that utilizes four different S. typhimurium strains (TA98, TA100, TA1535, TA1537) which possess unique mutations within the histidine operon.[38] Compounds that induce reverse mutations allow these strains to grow in the absence of histidine which is measured spectroscopically. The S. typhimurium strain TA1535 contains a T to C missense mutation in the hisG gene (his G46) leading to a leucine to proline amino acid substitution. With the reversal of this mutation, TA1535 can detect compounds that cause base pair mutations. The TA1537 strain detects compounds that induce a +1 frameshift mutation on the his C gene (his C3076). This allows frameshift mutagens to be detected. The TA98 strain detects +1 frameshift mutation on the his D gene (his D3052) and also contains the pkM101 plasmid, which increases the sensitivity of the strain to mutagenic compounds. Finally, TA100 contains the same mutation as TA1535 plus the pkM101 plasmid. The Ames fluctuation test also employs rat liver enzyme fractions (S9) to assess the potential mutagenicity of metabolites produced by the action of the liver enzymes on the test compound.

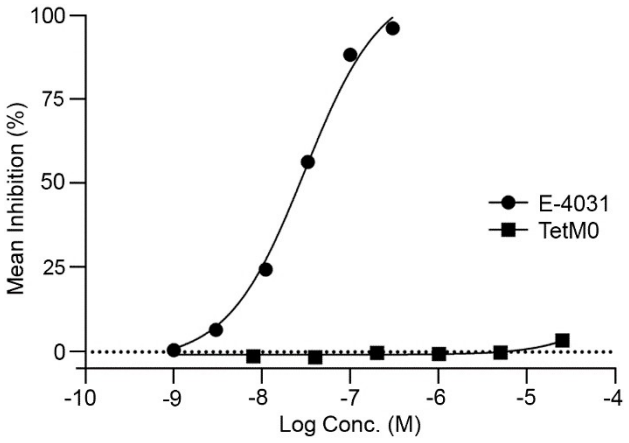

Figure 7. TetM0 does not inhibit the hERG ion channel. The hERG assay was conducted using HEK 293 stably transfected with hERG cDNA in an automated QPatch HTX patch clamp study. Plot of mean hERG ion channel inhibition (%, $n = 3$–4) versus log concentration for E-4031 (•) and **TetM0** (γ).

Initially, bacterial cytotoxicity assays were performed to determine whether **TetM0** was cytotoxic toward the histidine revertant tester strains (TA98R, TA100R, TA1535R, TA1537R) which would cause false negatives in the Ames fluctuation test. For this purpose, the four tester strains were cultured overnight at 37 °C in media containing Davis Mingoli salts, D-glucose, D-biotin, and low level histidine at pH 7.0 yielding OD_{650} from 0.60 to 1.10. The cultures were then incubated with eight different concentrations of **TetM0** (0.6, 1.2, 2.5, 5, 10, 25, 50, 100 μM; $n = 3$) for 96 h followed by measurement of OD_{650}. Compounds that exhibit OD_{650} values less than 60% of control (not treated with compound) are deemed cytotoxic and do not proceed to the Ames fluctuation test. The known cytotoxic compound mitomycin C ($IC_{50} \leq 100$ nM toward the tester strains) is used as a positive control. **TetM0** did not exhibit bacterial cytotoxicity toward any of the four tester strains at concentrations up to 100 μM (Supporting Information).

Given the absence of bacterial cytotoxicity for **TetM0**, the Ames fluctuation test was subsequently performed. For this purpose, the four tester strains of bacteria were cultured overnight in media containing Davis Mingoli salts, D-glucose, D-biotin, and low level histidine at pH 7.0 yielding OD_{650} from 0.60 to 1.10. The cultures were then incubated in the absence of **TetM0** or in the presence of **TetM0** (5, 10, 50, 100 μM; n = 48) both with and without Arochlor-induced rat liver S9 fraction (0.2 mg mL^{-1}) for 96 h. Bromocresol purple is included as a colorimetric pH indicator that responds to the pH drop resulting from bacterial growth upon reverse mutation. After 96 h, the OD_{430} and OD_{570} values are measured and the number of positive wells with $OD_{430}/OD_{570} \geq 1$ is determined as surrogate for reverse mutation. The significance of the number of positive wells in the treatment groups (**TetM0** present) versus the control group (**TetM0** absent) is calculated using the one-tailed Fisher's exact test and classified as follows: $p < 0.001$ (very strong positive, +++); $0.001 < p < 0.01$ (strong positive, ++); $0.01 < p < 0.05$ (weak positive, +); $p > 0.05$ (negative, −). Control compounds known to induce reverse mutation [2-aminoanthracene (2-AA), 9-aminoacridine (9-AA), Quercetin (Quer.), Streptozotocin (Strept.)] were tested as positive controls. Table 2 presents the results of the Ames fluctuation test. As can be readily seen, compared to background, none of the **TetM0** treatments result in a statistically significant increase in the number of positive wells. This indicates that **TetM0** does not significantly increase the rate of reverse mutation and is not genotoxic. Conversely, the genotoxic control compounds

Table 2. Results from the Ames fluctuation test conducted for **TetM0**.

TetM0 [μM]	TA98 −S9	TA98 +S9	TA100 −S9	TA100 +S9	TA1535 −S9	TA1535 +S9	TA1537 −S9	TA1537 +S9
0	0/48	1/48	0/48	4/48	0/48	0/48	1/48	0/48
5	0/48	0/48	0/48	4/48	0/48	0/48	0/48	0/48
	−	−	−	−	−	−	−	−
10	0/48	0/48	0/48	0/48	0/48	0/48	0/48	1/48
	−	−	−	−	−	−	−	−
50	0/48	0/48	0/48	5/48	0/48	0/48	0/48	1/48
	−	−	−	−	−	−	−	−
100	0/48	2/48	2/48	1/48	0/48	0/48	0/48	0/48
	−	−	−	−	−	−	−	−
Strept.	0/48	0/48	5/48	7/48	16/48	24/48	1/48	1/48
	−	−	+	−	+++	+++	−	−
2-AA	0/48	13/48	0/48	11/48	0/48	9/48	0/48	6/48
	−	+++	−	+	−	++	−	+
Quer.	5/48	10/48	0/48	5/48	1/48	0/48	1/48	5/48
	+	+++	−	−	−	−	−	+
9-AA	0/48	0/48	0/48	2/48	0/48	0/48	24/48	24/48
	−	−	−	−	−	−	+++	+++

Streptozotocin, 2-AA, Quercetin, and 9-AA all display the expected increase in genotoxicity in one or more bacterial strains.

Treatment with TetM0 controls the hyperlocomotion of mice treated with methamphetamine

Given the high affinity of the **TetM0**·methamphetamine complex ($K_a = 2.49 \times 10^6\ M^{-1}$) and its encouraging toxicology profile, we investigated whether **TetM0** could be used to sequester methamphetamine in vivo and thereby control its biological effects. For this purpose, we took advantage of the hyperlocomotive effects seen in mice treated with methamphetamine (0.5 mg/kg)[39] which can be monitored using an open-field test.[40] A total of 15 Swiss Webster mice were surgically implanted with jugular catheters with head mounted ports as described previously (Supporting Information).[28] Following surgery, mice were placed in the behavioral arena (day 1) to establish baseline locomotion levels before treatment began (Figure 8). Six additional daily sessions (days 2–7) were conducted using a semi-counterbalanced design where each mouse received one of six experimental treatments (D5 W only, **TetM0** only, methamphetamine only, a premixed solution of **TetM0** and methamphetamine, **TetM0** followed 30 s later by methamphetamine (prevention), and methamphetamine followed 30 s later by **TetM0** (treatment)) each day. For each experiment, total locomotion counts (i.e., the total number of beam breaks) were obtained for each mouse across the entirety of each training session. For each experiment, locomotion counts were then analyzed across treatments using one-way repeated measures ANOVA with Tukey-corrected pairwise post-hoc t-tests in Graphpad Prism and the results are presented in Figure 8. Mixed effects analysis revealed a significant main effect of treatment ($F(6,84) = 44.43$, $p = 0.0001$) with Tukey-corrected post-hoc comparison showing a significant increase in locomotion counts for treatment with methamphetamine against all other treatments (p's < 0.05). Importantly, there is no statistically significant difference between the locomotion counts seen for the baseline, D5 W only, **TetM0** only treatments which establishes that **TetM0** treatment does not affect locomotion. The locomotion counts for these three treatments are statistically significantly different ($p < 0.0001$) than that of the methamphetamine only treatment. Mice treated with a premixed solution of **TetM0** and methamphetamine (11.6:1) displayed locomotion counts there are statistically significantly smaller than methamphetamine treatment ($p < 0.0001$) and in fact are comparable to baseline locomotion counts. Precomplexation of methamphetamine by **TetM0** in the syringe effectively prevents the biological action of methamphetamine in the mice. The results of treatment with **TetM0** 30 seconds before treatment with methamphetamine allows us to address whether the molecular recognition of methamphetamine by **TetM0** also occurs in the biological setting. Figure 8 shows that the locomotion count for the 30s prevention group is much lower ($p < 0.0001$) than methamphetamine alone and is comparable to baseline locomotion levels which establishes that hyperlocomotion can be prevented by prior administration of **TetM0**. Finally, when mice were given methamphetamine 30 seconds before **TetM0**, we find that the locomotion levels are statistically significantly lower than that of methamphetamine alone ($p < 0.001$). Post-facto treatment with **TetM0** is effective at controlling hyperlocomotion. However, it should be noted that the locomotion counts for the 30s treatment condition is statistically significantly higher than the other groups (p from 0.0002 to 0.0153) which suggests incomplete sequestration of methamphetamine by **TetM0** under these conditions.

Although the results presented in Figure 8 suggest that **TetM0** sequesters methamphetamine and induces behavioral change, it is possible that the 30s interval between methamphetamine administration and **TetM0** administration in the reversal condition is too short to be ethologically relevant. To address this issue, we conducted a follow up experiment on days 8 and 9 of testing, where mice ($n = 15$) were administered either methamphetamine followed by administration of D5 W 5 minutes later or methamphetamine followed by **TetM0** (6 mM

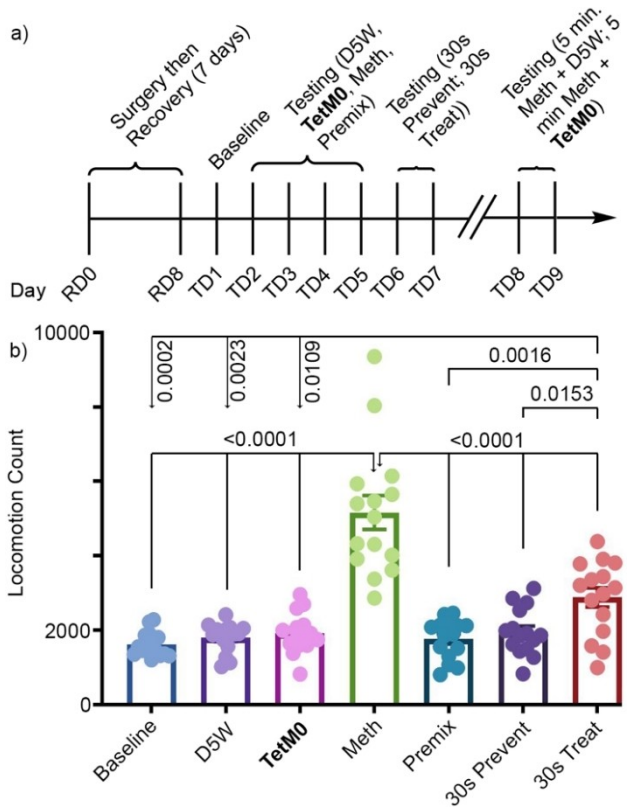

Figure 8. In vivo reversal of methamphetamine-induced hyperlocomotion by **TetM0**. a) Testing schedule. b) Average locomotion counts for male Swiss Webster mice ($n = 15$; avg weight (g) ± SD: 33.27 ± 1.44) are plotted as a function of treatment. All mice underwent an initial habituation to determine baseline locomotion levels before treatment. Following this baseline measure, treatment order was counterbalanced across days, and mice only received one treatment per day. Over six consecutive days of testing mice each received a single treatment of 5% aqueous dextrose (D5 W; 0.2 mL infused), **TetM0** only (**TetM0**; 6 mM in D5 W; 0.178 mL infused), methamphetamine only (4.24 mM methamphetamine in D5 W; 0.5 mg/kg; 0.022 mL infused), a premixed solution of **TetM0** and methamphetamine (Premix; ~11.6:1 **TetM0**:methamphetamine; 0.2 mL infused), **TetM0** followed by methamphetamine administered 30 s later (30s Blocking; 0.178 mL of 6 mM **TetM0** in D5 W, 0.022 mL of 4.24 mM methamphetamine in D5 W infused), and methamphetamine followed by **TetM0** administered 30 s later (30 s Reversal; 0.022 mL of 4.24 mM methamphetamine in D5 W, 0.178 mL of 6 mM **TetM0** in D5 W infused). Bars represent average locomotion counts. Error bars represent the standard error of the mean (SEM). Dots represent counts for each mouse ($n = 15$). Presented p-values are only for significant ($p < 0.05$) Tukey-corrected post-hoc comparisons.

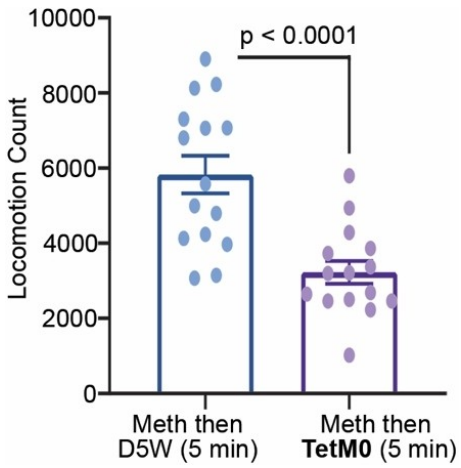

Figure 9. In vivo reversal of methamphetamine-induced hyperlocomotion by **TetM0** following 5-minute inter-injection interval. Average locomotion counts for male Swiss Webster mice ($n = 15$; avg weight (g) ± SD: 33.27 ± 1.44) are plotted as a function of treatment. Mice receive methamphetamine (4.24 mM methamphetamine in D5 W; 0.5 mg/kg; 0.022 mL infused) followed by either D5 W (0.178 mL infused) or **TetM0** (6 mM in D5 W; 0.178 mL infused) administered 5 minutes later before being placed into the behavioral box. Bars represent average locomotion counts. Error bars represent the standard error of the mean (SEM). Dots represent counts for each mouse ($n = 15$). Data analyzed using a paired t-test.

in D5 W) 5 minutes later in a counterbalanced manner before being placed in the open field. Figure 9 plots locomotion counts as a function of each treatment. We observed a statistically significant decrease in locomotion when **TetM0** was administered 5 minutes after methamphetamine compared to when D5 W was administered 5 minutes after methamphetamine (paired t-test, $t(14) = 8.282$, $p = 0.0001$). Although not directly comparable from an experimental design perspective, importantly locomotion levels in the 5-minute reversal using **TetM0** closely approximate those observed in control conditions on Day 1–7, while locomotion counts in the D5 W condition appear to approximate those observed with the methamphetamine only treatment. Collectively these findings firmly establish that **TetM0** is capable of sequestering methamphetamine in vivo and reversing methamphetamine-induced hyperlocomotion, with little to no effect on the locomotor behavior of the animal itself.

Conclusion

In summary, we have synthesized two new sulfated acyclic CB[n]-type receptors (**TriM0** and **Me_4TetM0**) which do not undergo self-association in aqueous solution which enables their binding toward guest molecules. We used complexation induced changes in ^{1}H NMR chemical shift to glean information on the geometry and dynamics of the host–drug complexes. We find that hydrophobic moieties of the drug is bound within the cavity of the acyclic CB[n]-type receptor whereas the cationic N-atom resides at the ureidyl C=O portal. Binding thermodynamics for the complexes between hosts **TetM0**, **TriM0**, and **Me_4TetM0** with drugs of abuse **1–13** were measured by direct ITC titrations. The conserved (substituted) phenylammonium ion unit of methamphetamine, fentanyl, MDMA and mephedrone constitutes a privileged binding site for **TetM0** with K_a values exceeding 10^6 M^{-1}. **TetM0** displays low in vitro cytotoxicity below 100 μM toward HEK 293 and HepG2 cells according to standard MTS metabolic and AK release cell death assays and no deleterious effects in maximum tolerated dose studies in mice up to 6 mM. **TetM0** does not inhibit the hERG ion channel and is not mutagenic according to the Ames fluctuation test. Finally, in vivo efficacy studies showed that methamphetamine induced hyperlocomotion can be effectively controlled by post-facto treatment with **TetM0** up to 5 minutes

later. Taken as a whole, the work establishes that sulfated acyclic CB[n]-type receptors have great potential as broad spectrum in vivo sequestering agents.

Acknowledgements

We thank the National Institutes of Health (GM132345) for financial support. We thank the Drug Supply Program of the National Institute on Drug Abuse for samples of the drugs used in this study. M.S. thanks the NIH (T32GM080201) for a training grant fellowship. S.M. thanks the University of Maryland for summer research and Department of Education GAANN (P200A150033) fellowships.

Conflict of Interest

L.I. is an inventor on patents filed by the University of Maryland on the biomedical application of acyclic CB[n]-type receptors.

Keywords: cucurbituril · hyperlocomotion · methamphetamine · molecular recognition · sequestration agents

[1] Facing Addition in America: The Surgeon General's Report on Alcohol, Drugs, and Health, 2016 https:// >www.surgeongeneral.gov/library/2016alcoholdrugshealth/index.html (accessed April 6, **2017**).
[2] a) Behavioral Health Trends in the United States. https://www.samhsa.gov/data/sites/default/files/NSDUH-FRR1-2014/NSDUH-FRR1-2014.pdf (accessed October 1, 2021; b) National Drug Threat Assessment 2011. www.justice.gov/archive/ndic/pubs44/44849/44849p.pdf (accessed April 6, 2017); c) H. G. Birnbaum, A. G. White, M. Schiller, T. Waldman, J. M. Cleveland, C. L. Roland, *Pain Medicine* **2011**, *12*, 657–667; d) C. S. Florence, C. Zhou, F. Luo, L. Xu, *Medical Care* **2013**, *54*, 901–906.
[3] D. A. Gorelick, *Future Med. Chem.* **2012**, *4*, 227–243.
[4] P. Skolnick, *Trends Pharmacol. Sci.* **2015**, *36*, 628–635.
[5] a) R. Rzasa Lynn, J. Galinkin, *Ther. Adv. Drug Saf.* **2018**, *9*, 63–88; b) R. B. Moss, D. J. Carlo, *Subst. Abuse Treat. Prev. Policy* **2019**, *14*, 6.
[6] a) C.-G. Zhan, F. Zheng, D. W. Landry, *J. Am. Chem. Soc.* **2003**, *125*, 2462–2474; b) F. Zheng, W. Yang, M.-C. Ko, J. Liu, H. Cho, D. Gao, M. Tong, H.-H. Tai, J. H. Woods, C.-G. Zhan, *J. Am. Chem. Soc.* **2008**, *130*, 12148–12155; c) M. J. Shram, O. Cohen-Barak, B. Chakraborty, M. Bassan, K. A. Schoedel, H. Hallak, E. Eyal, S. Weiss, Y. Gilgun, E. M. Sellers, J. Faulknor, O. Spiegelstein, *J. Clin. Psychopharmacol.* **2015**, *35*, 396–405.
[7] a) T. R. Kosten, C. B. Domingo, D. Shorter, F. Orson, C. Green, E. Somoza, R. Sekerka, F. R. Levin, J. J. Mariani, M. Stitzer, D. A. Tompkins, J. Rotrosen, V. Thakkar, B. Smoak, K. Kampman, *Drug Alcohol Depend.* **2014**, *140*, 42–47; b) M. W. Stevens, R. L. Henry, S. M. Owens, R. Schutz, W. B. Gentry, *mAbs* **2014**, *6*, 1649–1656; c) P. T. Bremer, A. Kimishima, J. E. Schlosburg, B. Zhou, K. C. Collins, K. D. Janda, *Angew. Chem. Int. Ed.* **2016**, *55*, 3772–3775; *Angew. Chem.* **2016**, *128*, 3836–3839; d) K. C. Collins, J. E. Schlosburg, P. T. Bremer, K. D. Janda, *J. Med. Chem.* **2016**, *59*, 3878–3885; e) A. Kimishima, C. J. Wenthur, L. M. Eubanks, S. Sato, K. D. Janda, *Mol. Pharmaceutics* **2016**, *13*, 3884–3890; f) M. Gooyit, P. O. Miranda, C. J. Wenthur, A. Ducime, K. D. Janda, *ACS Chem. Neurosci.* **2017**, *8*, 468–472.
[8] a) S. Ganapati, S. D. Grabitz, S. Murkli, F. Scheffenbichler, M. I. Rudolph, P. Y. Zavalij, M. Eikermann, L. Isaacs, *ChemBioChem* **2017**, *18*, 1583–1588; b) C.-L. Deng, S. L. Murkli, L. D. Isaacs, *Chem. Soc. Rev.* **2020**, *49*, 7516–7532; c) H. Yin, X. Zhang, J. Wei, S. Lu, D. Bardelang, R. Wang, *Theranostics* **2021**, *11*, 1513–1526; d) A. Bom, M. Bradley, K. Cameron, J. K. Clark, J. Van Egmond, H. Feilden, E. J. MacLean, A. W. Muir, R. Palin, D. C. Rees, M.-Q. Zhang, *Angew. Chem. Int. Ed.* **2002**, *41*, 265–270 Angew. Chem. **2002**, 114, 275–280.
[9] a) J.-M. Lehn, *Angew. Chem. Int. Ed. Engl.* **1988**, *27*, 89–112; *Angew. Chem.* **1988**, *100*, 91–116; b) C. J. Pedersen, *Angew. Chem. Int. Ed. Engl.* **1988**, *27*, 1021–1027; *Angew. Chem.* **1988**, *100*, 1053–1059; c) D. J. Cram, *Angew. Chem. Int. Ed. Engl.* **1988**, *27*, 1009–1020; *Angew. Chem.* **1988**, *100*, 1041–1052; d) J. F. Stoddart, *Angew. Chem. Int. Ed.* **2017**, *56*, 11094–11125 Angew. Chem. **2017**, 129, 11244–11277.
[10] a) M. V. Rekharsky, Y. Inoue, *Chem. Rev.* **1998**, *98*, 1875–1917; b) C. D. Gutsche, *Acc. Chem. Res.* **1983**, *16*, 161–170; c) F. Diederich, *Angew. Chem. Int. Ed. Engl.* **1988**, *27*, 362–386; *Angew. Chem.* **1988**, *100*, 372–396; d) J. Murray, K. Kim, T. Ogoshi, W. Yao, B. C. Gibb, *Chem. Soc. Rev.* **2017**, *46*, 2479–2496; e) T. Ogoshi, T.-A. Yamagishi, Y. Nakamoto, *Chem. Rev.* **2016**, *116*, 7937–8002; f) M. Xue, Y. Yang, X. Chi, Z. Zhang, F. Huang, *Acc. Chem. Res.* **2012**, *45*, 1294–1308; g) R. A. Rajewski, V. J. Stella, *J. Pharm. Sci.* **1996**, *85*, 1142–1169; h) S. J. Barrow, S. Kasera, M. J. Rowland, J. del Barrio, O. A. Scherman, *Chem. Rev.* **2015**, *115*, 12320–12406; i) V. Boehmer, *Angew. Chem. Int. Ed. Engl.* **1995**, *34*, 713–745; *Angew. Chem.* **1995**, *107*, 785–818.
[11] a) G. Ghale, W. M. Nau, *Acc. Chem. Res.* **2014**, *47*, 2150–2159; b) M. K. Meadows, E. V. Anslyn, *Macrocyclic Supramol. Chem.* **2016**, 92–126; c) B. Daly, T. S. Moody, A. J. M. Huxley, C. Yao, B. Schazmann, A. Alves-Areias, J. F. Malone, H. Q. N. Gunaratne, P. Nockemann, A. P. de Silva, *Nat. Commun.* **2019**, *10*, 1–7.
[12] a) Y. Ueda, H. Ito, D. Fujita, M. Fujita, *J. Am. Chem. Soc.* **2017**, *139*, 6090–6093; b) S. H. A. M. Leenders, R. Gramage-Doria, B. de Bruin, J. N. H. Reek, *Chem. Soc. Rev.* **2015**, *44*, 433–448; c) C. J. Brown, F. D. Toste, R. G. Bergman, K. N. Raymond, *Chem. Rev.* **2015**, *115*, 3012–3035.
[13] a) J. A. McCune, S. Mommer, C. C. Parkins, O. A. Scherman, *Adv. Mater.* **2020**, *32*, 1906890; b) D. Xia, P. Wang, X. Ji, N. M. Khashab, J. L. Sessler, F. Huang, *Chem. Rev.* **2020**, *120*, 6070-6123.
[14] R. Sardella, F. Ianni, M. Marinozzi, A. Macchiarulo, B. Natalini, *Curr. Med. Chem.* **2017**, *24*, 796–817.
[15] a) Aqdot Home Page. https://aqdot.com (accessed May 6, 2020); b) Febreze Home Page. https://www.febreze.com/en-us (accessed May 5, 2020).
[16] a) Y. H. Ko, E. Kim, I. Hwang, K. Kim, *Chem. Commun.* **2007**, 1305–1315; b) S. Kassem, T. van Leeuwen, A. S. Lubbe, M. R. Wilson, B. L. Feringa, D. A. Leigh, *Chem. Soc. Rev.* **2017**, *46*, 2592–2621.
[17] a) K. Wang, D.-S. Guo, H.-Q. Zhang, D. Li, X.-L. Zheng, Y. Liu, *J. Med. Chem.* **2009**, *52*, 6402–6412; b) D.-S. Guo, Y. Liu, *Acc. Chem. Res.* **2014**, *47*, 1925–1934.
[18] a) X. Zhang, Q. Cheng, L. Li, L. Shangguan, C. Li, S. Li, F. Huang, J. Zhang, R. Wang, *Theranostics* **2019**, *9*, 3107–3121; b) D. N. Shurpik, O. A. Mostovaya, D. A. Sevastyanov, O. A. Oksana, A. S. Sapunova, A. D. Voloshina, K. A. Petrov, I. V. Kovyazina, P. J. Cragg, I. I. Stoikov, *Org. Biomol. Chem.* **2019**, *17*, 9951–9959; c) L. Shangguan, Q. Chen, B. Shi, F. Huang, *Chem. Commun.* **2017**, *53*, 9749–9752.
[19] a) J. M. Dempsey, C. Zhai, H. H. McGarraugh, C. L. Schreiber, S. E. Stoffel, A. Johnson, B. D. Smith, *Chem. Commun.* **2019**, *55*, 12793–12796; b) C. L. Schreiber, B. D. Smith, *Nat. Chem. Rev.* **2019**, *3*, 393–400.
[20] V. J. Stella, R. A. Rajewski, *Pharm. Res.* **1997**, *14*, 556–567.
[21] J. M. Adam, D. J. Bennett, A. Bom, J. K. Clark, H. Feilden, E. J. Hutchinson, R. Palin, A. Prosser, D. C. Rees, G. M. Rosair, D. Stevenson, G. J. Tarver, M.-Q. Zhang, *J. Med. Chem.* **2002**, *45*, 1806–1816.
[22] a) D. Shetty, J. K. Khedkar, K. M. Park, K. Kim, *Chem. Soc. Rev.* **2015**, *44*, 8747–8761; b) K. I. Assaf, W. M. Nau, *Chem. Soc. Rev.* **2015**, *44*, 394–418; c) E. Masson, X. Ling, R. Joseph, L. Kyeremeh-Mensah, X. Lu, *RSC Adv.* **2012**, *2*, 1213–1247.
[23] a) W. L. Mock, N.-Y. Shih, *J. Org. Chem.* **1986**, *51*, 4440–4446; b) S. Liu, C. Ruspic, P. Mukhopadhyay, S. Chakrabarti, P. Y. Zavalij, L. Isaacs, *J. Am. Chem. Soc.* **2005**, *127*, 15959–15967; c) L. Cao, M. Sekutor, P. Y. Zavalij, K. Mlinaric-Majerski, R. Glaser, L. Isaacs, *Angew. Chem. Int. Ed.* **2014**, *53*, 988–993; *Angew. Chem.* **2014**, *126*, 1006–1011; d) M. V. Rekharsky, T. Mori, C. Yang, Y. H. Ko, N. Selvapalam, H. Kim, D. Sobransingh, A. E. Kaifer, S. Liu, L. Isaacs, W. Chen, S. Moghaddam, M. K. Gilson, K. Kim, Y. Inoue, *Proc. Natl. Acad. Sci. USA* **2007**, *104*, 20737–20742.
[24] a) V. D. Uzunova, C. Cullinane, K. Brix, W. M. Nau, A. I. Day, *Org. Biomol. Chem.* **2010**, *8*, 2037–2042; b) X. Zhang, X. Xu, S. Li, L.-H. Wang, J. Zhang, R. Wang, *Sci. Rep.* **2018**, *8*, 1–7.
[25] X. Zhang, X. Xu, S. Li, L. Li, J. Zhang, R. Wang, *Theranostics* **2019**, *9*, 633–645.
[26] Q. Huang, Q. Cheng, X. Zhang, H. Yin, L.-H. Wang, R. Wang, *ACS Appl. Bio Mater.* **2018**, *1*, 544–548.
[27] H. Chen, J. Y. W. Chan, S. Li, J. J. Liu, I. W. Wyman, S. M. Y. Lee, D. H. Macartney, R. Wang, *RSC Adv.* **2015**, *5*, 63745–63752.

[28] S. Murkli, J. Klemm, A. T. Brockett, M. Shuster, V. Briken, M. R. Roesch, L. Isaacs, *Chem. Eur. J.* **2021**, *27*, 3098–3105.
[29] a) S. Ganapati, L. Isaacs, *Isr. J. Chem.* **2018**, *58*, 250–263; b) D. Bauer, B. Andrae, P. Gass, D. Trenz, S. Becker, S. Kubik, *Org. Chem. Front.* **2019**, *6*, 1555-1560; c) D. Mao, Y. Liang, Y. Liu, X. Zhou, J. Ma, B. Jiang, J. Liu, D. Ma, *Angew. Chem. Int. Ed.* **2017**, *41*, 12614–12618; *Angew. Chem.* **2017**, *129*, 12788–12792.
[30] a) L. Gilberg, B. Zhang, P. Y. Zavalij, V. Sindelar, L. Isaacs, *Org. Biomol. Chem.* **2015**, *13*, 4041–4050; b) B. Zhang, L. Isaacs, *J. Med. Chem.* **2014**, *57*, 9554–9563; c) B. Zhang, P. Y. Zavalij, L. Isaacs, *Org. Biomol. Chem.* **2014**, *12*, 2413–2422.
[31] a) D. Ma, B. Zhang, U. Hoffmann, M. G. Sundrup, M. Eikermann, L. Isaacs, *Angew. Chem. Int. Ed.* **2012**, *51*, 11358–11362; *Angew. Chem.* **2012**, *124*, 11520–11524; b) D. Diaz-Gil, F. Haerter, S. Falcinelli, S. Ganapati, G. K. Hettiarachchi, J. C. P. Simons, B. Zhang, S. D. Grabitz, I. M. Duarte, J. F. Cotten, K. Eikermann-Haerter, H. Deng, N. L. Chamberlin, L. Isaacs, V. Briken, M. Eikermann, *Anesthesiology* **2016**, *125*, 333–345; c) T. Thevathasan, S. D. Grabitz, P. Santer, P. Rostin, O. Akeju, J. D. Boghosian, M. Gill, L. Isaacs, J. F. Cotton, M. Eikermann, *Br. J. Anaesth.* **2020**, *125*, E140–E147.
[32] X. Lu, S. A. Zebaze Ndendjio, P. Y. Zavalij, L. Isaacs, *Org. Lett.* **2020**, *22*, 4833–4837.
[33] T. Wiseman, S. Williston, J. F. Brandts, L.-N. Lin, *Anal. Biochem.* **1989**, *179*, 131–137.
[34] J. Broecker, C. Vargas, S. Keller, *Anal. Biochem.* **2011**, *418*, 307–309.
[35] a) E. Persch, O. Dumele, F. Diederich, *Angew. Chem. Int. Ed.* **2015**, *54*, 3290–3327; *Angew. Chem.* **2015**, *127*, 3341–3382; b) F. Biedermann, V. D. Uzunova, O. A. Scherman, W. M. Nau, A. De Simone, *J. Am. Chem. Soc.* **2012**, *134*, 15318–15323.
[36] D. C. Bell, B. Fermini, *J. Pharmacol. Toxicol. Methods* **2021**, *110*, 107072.
[37] O. Roche, G. Trube, J. Zuegge, P. Pflimlin, A. Alanine, G. Schneider, *ChemBi°Chem* **2002**, *3*, 455–459.
[38] a) B. A. Bridges, *Arch. Toxicol.* **1980**, *46*, 41–44; b) M. Kamber, S. Fluckiger-Isler, G. Engelhardt, R. Jaeckh, E. Zeiger, *Mutagenesis* **2009**, *24*, 359–366.
[39] a) A. L. Sharp, E. Varela, L. Bettinger, M. J. Beckstead, *Int. J. Neuropsychopharmacol.* **2015**, *18*, 1–10; b) R. A. K. Singh, T. A. Kosten, B. M. Kinsey, X. Shen, A. Y. Lopez, T. R. Kosten, F. M. Orson, *Pharmacol. Biochem. Behav.* **2012**, *103*, 230–236.
[40] R. N. Walsh, R. A. Cummins, *Psychological Bulletin* **1976**, *83*, 482–504.

Manuscript received: August 10, 2021
Accepted manuscript online: October 6, 2021
Version of record online: October 27, 2021